Tank-treading, swinging, and tumbling of liquid-filled elastic capsules in shear flow

Y. Sui,[1] H. T. Low,[2] Y. T. Chew,[1] and P. Roy[2]
[1]*Laboratory of Fluid Mechanics, Department of Mechanical Engineering, National University of Singapore, Singapore 119260*
[2]*Division of Bioengineering, National University of Singapore, Singapore 119260*

(Received 3 September 2007; revised manuscript received 13 November 2007; published 31 January 2008)

The dynamic motion of three-dimensional (3D) capsules in a shear flow is investigated by direct numerical simulation. The capsules are modeled as Newtonian liquid droplets enclosed by elastic membranes, with or without considering the membrane-area incompressibility. The internal liquid of the capsules is the same as that outside. The dynamic motion of capsules with initially spherical and oblate spheroidal unstressed shapes is studied under various shear rates. The results show that spherical capsules deform to stationary configurations and then the membranes rotate around the liquid inside (steady tank-treading motion). Such a steady mode is not observed for oblate spheroidal capsules. It is shown that with the shear rate decreasing, the motion of oblate spheroidal capsules changes from the swinging mode (a capsule undergoes periodic shape deformation and inclination oscillation while its membrane is rotating around the liquid inside) to tumbling mode.

DOI: 10.1103/PhysRevE.77.016310 PACS number(s): 47.55.−t, 47.63.−b

I. INTRODUCTION

Capsules consisting of thin elastic or incompressible membranes enclosing viscous Newtonian liquid are often employed as models for many kinds of particles, for example, biological cells, lipid vesicles. The flow-induced deformation of such capsules has been studied by many researchers in cellular biology, bioengineering, and chemical engineering. It is important in fundamental research, as well as in biomedical and industrial applications. Furthermore, it is the first step to model more complex situations which include capsule suspensions such as human microcirculation and cell filtration.

The dynamic motion of elastic capsules or vesicles under simple shear flow has been studied experimentally [1–5], theoretically [6–10], and numerically [11–17]. Vesicles are different from elastic capsules in that their membranes are incompressible and do not have shear elasticity. Two types of motion are well known: a steady tank-treading mode, in which a capsule deforms to a steady configuration then the membrane rotates around the liquid inside; an unsteady tumbling mode, in which a capsule flips continuously. Besides these two modes, a "swinging" mode has been observed in recent experiments for nonspherical capsules [4,5]. In this mode, with the membrane rotating around the liquid inside, the capsule undergoes periodic shape deformation and inclination oscillation. This mode has also been predicted theoretically [5,9,10] and numerically [11,16,17].

Which factors are important in determining a capsule's behavior is of great interests to researchers. It has been found that capsules immersed in a low viscosity fluid flip continuously, and capsules immersed in a fluid with sufficiently high viscosity carried out tank-treading motion. Keller and Skalak [8] theoretically analyzed the deformation of an ellipsoidal capsule in simple shear flow. It was found that for a capsule with a given geometry, the transition from tank-treading mode to tumbling mode depends on the viscosity ratio between internal fluid and external fluid, and it is independent of shear rate. This viscosity ratio-dependent transition has also been studied and explained in subsequent works [9,11,13]. Noguchi and Gompper [14,15] studied vesicles with viscous membrane and found that increasing the viscosity of membrane can also cause the mode transition. Sui *et al.* [17] recently studied the bending effect on deformation of capsules in shear flow by two-dimensional (2D) numerical simulation. It was found that for noncircular capsules, with bending energy at minimum at their initial shapes, an increase of bending stiffness can induce the transition from tank-treading mode to tumbling mode.

Recently, Walter *et al.* [4] studied synthetic microcapsules in shear flow by experiment. It is found that during the tank-treading motion of the membrane, the capsule undergoes periodic shape deformation and inclination oscillation; the inclination oscillation amplitude increases as the shear rate decreases. Similar motion has also been found on red blood cells in shear flow [5]: the cells present an oscillation of their inclination superimposed to the tank-treading motion, and the tank-treading-to-tumbling transition can be triggered by decreasing the shear rate. These experimental findings show that in shear flow, the dynamics of these capsules depend not only on viscosity ratio, but also on shear rate. Only recently, there are some pioneer analyses on these phenomena. Based on the theoretical model of Keller and Skalak [8], and under the assumption that the membrane elastic energy undergoes a periodic variation during the tank-treading motion, the above experimental findings can be successfully predicted by the theoretical analysis of Skotheim and Secomb [10], as well as Abkarian *et al.* [5]. In the theory of Skotheim and Secomb, the swinging-to-tumbling transition of an elastic capsule was found to occur via a narrow intermittent regime of successive swinging and tumbling. This has also been observed in the experiment of Abkarian *et al.* [5]. Noguchi and Gompper [16] numerically studied vesicles with viscous membranes. Their work is a numerical simulation which shows that there is a shear-rate–induced transition of vesicles' motion from swinging mode to tumbling mode. For liquid-filled capsules with elastic membrane, the shear-rate–induced transition of capsules' motion has not been reported in studies with direct

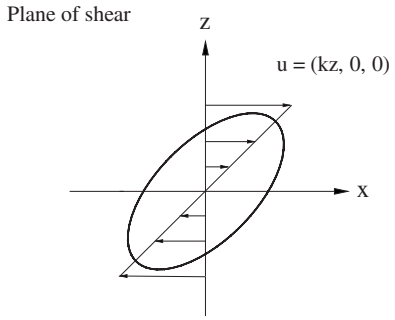

FIG. 1. Illustration of a capsule in a simple shear flow.

numerical simulation, which takes into account the deformation of the capsules.

In the present study, the dynamic motion of 3D capsules in shear flow is investigated by direct numerical simulation. The capsules are modeled as enclosed elastic membranes filled with Newtonian liquid the same as that outside. The capsule membrane is assumed to be infinite thin and the bending stiffness is neglected. The dynamic motion of spherical and oblate spheroidal capsules with both the neo-Hookean [11] and the Skalak [18] membrane constitutive laws is considered.

The present study is based on the hybrid method of Peng *et al.* [19] and Sui *et al.* [20]. The immersed boundary concept [21,22] was introduced into the framework of the lattice Boltzmann method [23–26]: The flow field was solved by the lattice Boltzmann method, and the fluid-capsule interaction was solved by the immersed boundary method. The multiblock strategy of Yu and Girimaji [27] was employed to refine the mesh around the deforming capsule, which substantially improved the accuracy and efficiency of the simulation. In the present paper, the hybrid method [20] is extended to 3D simulation. The capsule membrane is discretized into flat triangular elements. A finite element model [28,29] is employed to obtain the forces acting on the membrane nodes.

II. MODEL AND METHOD

A. Membrane laws

In the present study, the deformation of capsules is considered to be subjected to the incident shear flow along the x axis, $\mathbf{u}=(kz,0,0)$, as illustrated in Fig. 1. The membranes of the capsules are quite thin compared with the capsules' dimension, and are treated as 2D solid. Bending stiffness of the membranes is neglected.

In the present study, two different 2D membrane constitutive laws are employed. The simplest constitutive equation is the neo-Hookean (NH) law, here the formula of Ramanujan and Pozrikidis [11] is used. The strain energy function has the form

$$W^{NH} = \tfrac{1}{6}E\left[I_1 - \log(I_2+1) + \tfrac{1}{2}\log^2(I_2+1)\right], \qquad (1)$$

where E is the surface shear elasticity modulus, and I_1 and I_2 are the first and second strain invariants, with $I_1=\lambda_1^2+\lambda_2^2-2$, $I_2=(\lambda_1\lambda_2)^2-1$. The term λ_1 and λ_2 are the principle strains. The NH law corresponds to membranes made of polymerized material. The area dilation is unrestricted and is compensated by the thinning of the membrane.

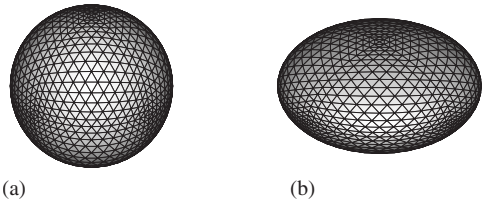

FIG. 2. Interfacial discretization of (a) a sphere; (b) an oblate spheroid with aspect ratio of 2:1.

Skalak *et al.* [18] proposed another law (SK) to model the membrane of red blood cells,

$$W^{SK} = \tfrac{1}{4}E\left(\tfrac{1}{2}I_1^2 + I_1 - I_2\right) + \tfrac{1}{8}CEI_2^2. \qquad (2)$$

On the right-hand side of the equation, the first term represents the shear effects and second term accounts for the area dilation. The term C is the ratio between area dilation modulus and shear elasticity modulus. It is quite large for incompressible biological membranes.

B. Finite element membrane model

In the present study, the 3D capsule membrane is discretized into flat triangular elements. The triangulation procedure is similar to that of Ramanujan and Pozrikidis [11]. To discretize the unstressed interface, each triangular face of a regular octahedron or icosahedron is subdivided into 4^n triangular elements. These elements are then projected radically onto a sphere. The geometry of each element is described by its three vertices. The discretization of a sphere surface is shown in Fig. 2(a). For oblate spheroid with aspect ratio b/a, the mapping system is stated as

$$x_{obl} = Rx, \quad y_{obl} = Ry, \quad z_{obl}(b/a)Rz, \qquad (3)$$

where the term R is the adjusting factor to keep the capsule volume. The surface discretization of an oblate spheroid with aspect ratio of 2:1 is shown in Fig. 2(b).

In the present study, the finite element membrane model developed by Charrier *et al.* [28] and Shrivastava *et al.* [29] is employed to obtain the forces acting at the discrete nodes of the membrane. In the finite element model, the membrane of the capsule is represented by a patchwork of flat triangular elements which remain flat after deformation, and the load on the membrane is represented by a concentrated load on the membrane nodes. Only in-plane stresses and strains exist. In the 3D deformation of the capsule, the membrane elements do not stay in the same plane after being displaced. In this model, the deformed element is transformed to the plane of the undeformed element, so that the relative displacement of the nodes and the corresponding forces are easily determined. The equations developed for the force exerted at the nodes of an element of the deformed membrane are given in the plane of the element.

The displacements are approximated by linear shape functions in the plane of the element with coordinates (x',y'). They are described by $\chi(x',y')=ax'+by'+c$. The unknown

coefficients a, b, and c are determined using known values of the displacements at the three nodes of the element. After the displacements of the three nodes of an element are known, its state of strain λ_1 and λ_2 can be obtained. The relation of membrane strain and membrane energy is governed by the constitutive law, which is determined by the membrane materials. With a constitutive law chosen, one can follow the usual finite element procedure and derive the relations between nodal forces and nodal displacements. The principle of virtual work is used to calculate the forces at the three nodes of an element. Because each node of the discrete membrane belongs to more than one element, the resultant force on a node is the sum of the forces exerted by all the elements attached to the node. So far, the force calculated is the fluid force acting on the capsule membrane. Its equal and opposite counterpart is the force acting on the fluid. It is distributed to the surrounding fluid by the approach described by the immersed boundary method.

Above is only a brief description of this model, the detailed treatment can be found in pertinent literatures [28,29].

C. Numerical method

The present study is based on a hybrid method [20], which is a combination of the immersed boundary method and the multiblock lattice Boltzmann method. The flow field was solved by the lattice Boltzmann method, and the fluid-capsule interaction was solved by the immersed boundary method. The multiblock strategy was employed to refine the mesh around the deforming capsule, which substantially improved the accuracy and efficiency of the simulation. In the present paper, the hybrid method is extended to 3D simulation.

In the immersed boundary method of Peskin [21,22], a force density is distributed to the Cartesian mesh in the vicinity of the moving boundary in order to account for the effect of the boundary. Two different sets of coordinate system are used. The fluid region is represented by Eulerian coordinates $\mathbf{x}$ and the moving boundary immersed in the fluid is represented by Lagrangian coordinates $\mathbf{s}$. Any position on the capsule membrane can be written as $\mathbf{x}=\mathbf{X}(\mathbf{s},t)$. The term $\mathbf{F}(\mathbf{s},t)$ represents the membrane force density, which is a combination of the internal link force induced by deformation and the external force. The term $\mathbf{f}(\mathbf{s},t)$ represents the fluid-body force density.

The nonslip boundary condition is satisfied by letting the flexible membrane move at the same velocity as the fluid around it, that is,

$$\frac{\partial \mathbf{X}(\mathbf{s},t)}{\partial t} = \mathbf{u}(\mathbf{X}(\mathbf{s},t),t). \tag{4}$$

This motion will cause the capsule to deform. The boundary force density $\mathbf{F}(\mathbf{s},t)$ is obtained from the constitutive law of the elastic membrane, and distributed to the fluid mesh points near it by a smoothed version of Dirac δ function, written as follows:

$$\mathbf{f}(\mathbf{x},t) = \int_{\Gamma} \mathbf{F}(\mathbf{s},t)\,\delta(\mathbf{x}-\mathbf{X}(\mathbf{s},t))d\mathbf{s}, \tag{5}$$

where

$$\delta(r) = \begin{cases} \frac{1}{4}\left[1+\cos\left(\frac{\pi|r|}{2}\right)\right], & r \leqslant 2, \\ 0, & r > 2, \end{cases} \tag{6}$$

in which r equals the distance between the Lagrange and Eulerian nodes divided by the Eulerian grid space. For the 3D case, the smoothed version of Dirac δ function can be written as

$$\delta(\mathbf{X}-\mathbf{X}_{ij}) = \delta(x-x_{ij})\,\delta(y-y_{ij})\,\delta(z-z_{ij}). \tag{7}$$

The same smoothed version of Dirac δ function is used to obtain the velocities of the Lagrangian nodes on the moving boundary.

The lattice Boltzmann method is a kinetic-based approach for simulating fluid flows. It decomposes the continuous fluid flow into pockets of fluid particles which can only stay at rest or move to one of the neighboring nodes. In the present study, the immersed boundary method is combined with the lattice Boltzmann method. In order to solve the flow field with a force density, the lattice Boltzmann equation (LBE) must be modified. Several forms of the LBE which can handle a force density have been proposed. Guo's approach [30] is more accurate for unsteady flow with force changing with time and space, in which the modified lattice Boltzmann equation is in the form of

$$f_i(\mathbf{x}+\mathbf{e}_i\Delta t, t+\Delta t) - f_i(\mathbf{x},t) = -\frac{1}{\tau}[f_i(\mathbf{x},t) - f_i^{eq}(\mathbf{x},t)] + \Delta t F_i, \tag{8}$$

where $f_i(\mathbf{x},t)$ is the distribution function for particles with velocity $\mathbf{e}_i$ at position $\mathbf{x}$ and time t, Δt is the lattice time interval, $f_i^{eq}(\mathbf{x},t)$ is the equilibrium distribution function, and τ is the nondimensional relaxation time.

The D3Q19 model is one of the most commonly used LB models for 3D simulation, the fluid particles have the possible discrete velocities stated as follows:

$$[\mathbf{e}_0,\mathbf{e}_1,\mathbf{e}_2,\mathbf{e}_3,\mathbf{e}_4,\mathbf{e}_5,\mathbf{e}_6,\mathbf{e}_7,\mathbf{e}_8,\mathbf{e}_9,\mathbf{e}_{10},\mathbf{e}_{11},\mathbf{e}_{12},\mathbf{e}_{13},\mathbf{e}_{14},\mathbf{e}_{15},\mathbf{e}_{16},\mathbf{e}_{17},\mathbf{e}_{18}]$$

$$= \begin{bmatrix} 0 & 1 & -1 & 0 & 0 & 0 & 0 & 1 & 1 & -1 & -1 & 1 & -1 & 1 & -1 & 0 & 0 & 0 & 0 \\ 0 & 0 & 0 & 1 & -1 & 0 & 0 & 1 & -1 & 1 & -1 & 0 & 0 & 0 & 0 & 1 & 1 & -1 & -1 \\ 0 & 0 & 0 & 0 & 0 & 1 & -1 & 0 & 0 & 0 & 0 & 1 & 1 & -1 & -1 & 1 & -1 & 1 & -1 \end{bmatrix}. \tag{9}$$

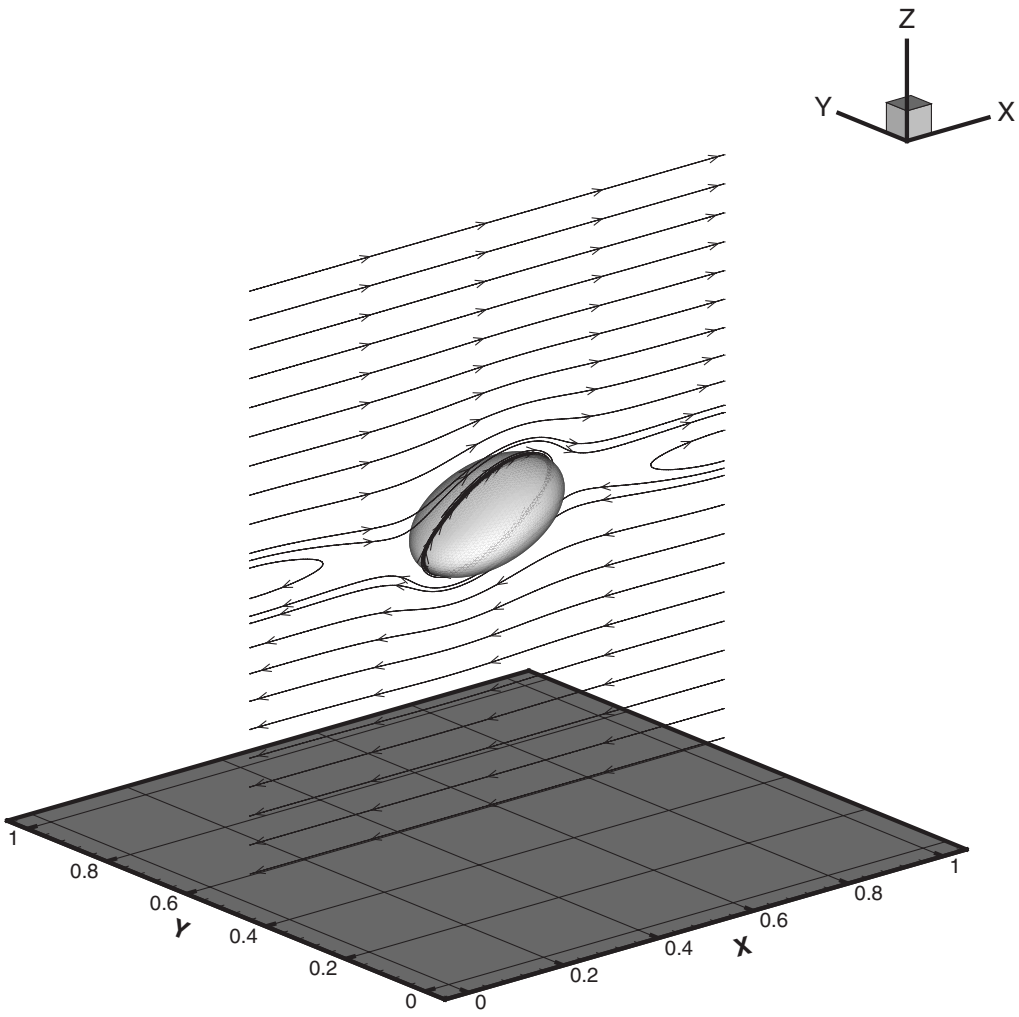

FIG. 3. Steady deformed capsule and the flow field around the cross section of the capsule in the plane of shear at $G=0.05$.

The equilibrium distribution function $f_i^{eq}(\mathbf{x},t)$ is in the form of

$$f_i^{eq} = E_i(\rho,\mathbf{u}) \tag{10}$$

$$\text{with} \quad E_i(\rho,\mathbf{u}) = \omega_i\rho\left(1+\frac{\mathbf{e}\cdot\mathbf{u}}{c_s^2}+\frac{\mathbf{uu}:(\mathbf{e}_i\mathbf{e}_i-c_s^2\mathbf{I})}{2c_s^4}\right), \tag{11}$$

where ω_i is the weighing factor, it equals $\frac{1}{3}$ for $i=0$, $\frac{1}{18}$ for $i=1-6$, and $\frac{1}{36}$ for $i=7-18$. The term c_s represents the sound speed, and equals $\Delta x/(\sqrt{3}\Delta t)$.

The relaxation time is related to the kinematic viscosity in Navier-Stokes equation in the form of

$$\nu = \left(\tau-\tfrac{1}{2}\right)c_s^2\Delta t. \tag{12}$$

The forcing term F_i is in the form of

$$F_i = \left(1-\frac{1}{2\tau}\right)\omega_i\left(\frac{\mathbf{e}_i-\mathbf{u}}{c_s^2}+\frac{(\mathbf{e}_i\cdot\mathbf{u})}{c_s^4}\mathbf{e}_i\right)\cdot\mathbf{f}. \tag{13}$$

Once the particle density distribution is known, the fluid density and momentum are calculated, using

$$\rho = \sum_i f_i, \quad \rho\mathbf{u} = \sum_i \mathbf{e}_i f_i + \tfrac{1}{2}\mathbf{f}\Delta t. \tag{14}$$

In the present paper, the multiblock lattice Boltzmann method proposed by Yu and Girimaji [27] is employed. The computational domain is divided into blocks which are connected through the interface. On the interface between blocks, the exchange of variables follows a certain relation so that the mass and momentum are conserved and the stress is continuous across the interface. Details can be found in pertinent reference [27].

In the present computation, a two-grid system is employed. The lattice space ratio between coarse and fine grids equals 2. The capsules are immersed in the fine mesh block. The present procedure for multiblock computation is very similar to that proposed by Yu and Girimaji [27]. The only difference exists in the computation on the fine mesh block. That is a subroutine implementing the immersed boundary method is added before the streaming and collision steps.

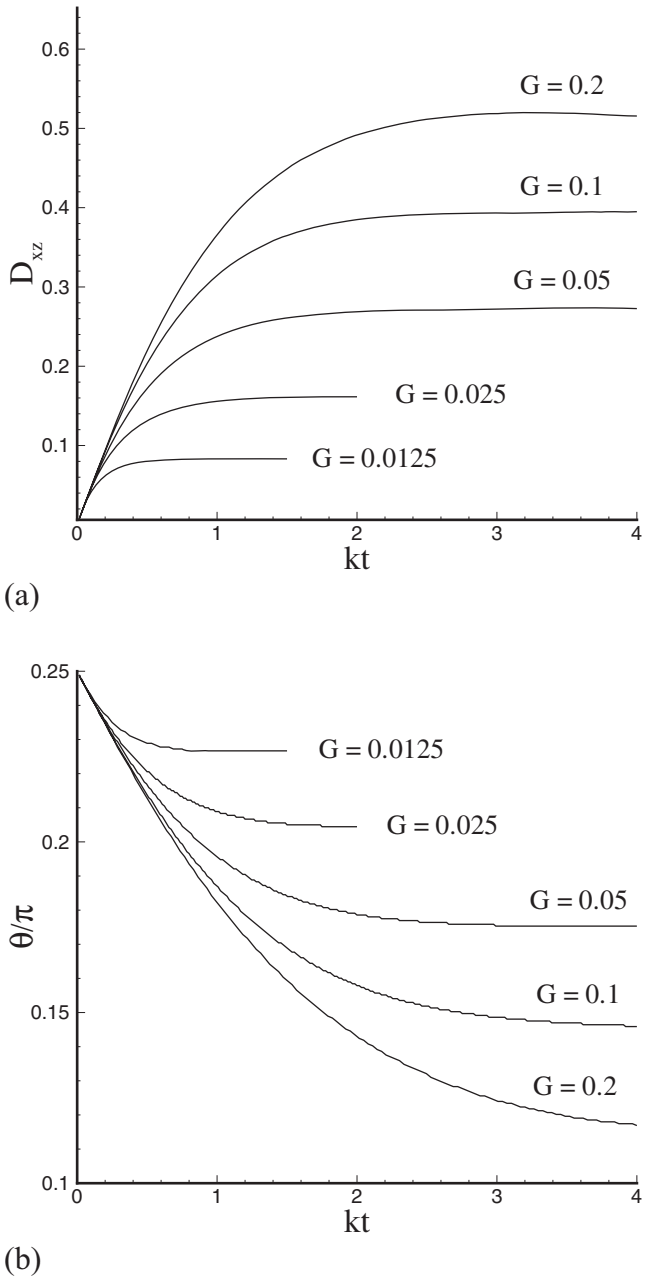

FIG. 4. Temporal evolutions of the (a) Taylor shape parameter and (b) inclination angle of the initially spherical capsules with NH membrane.

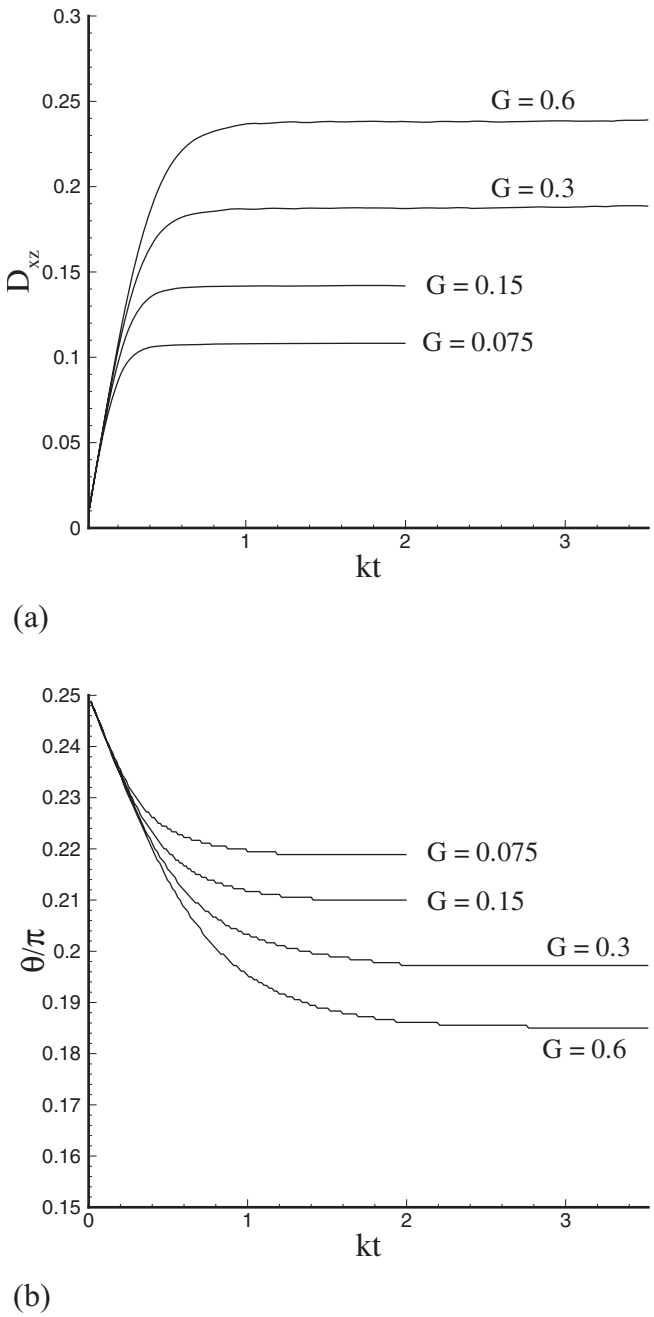

FIG. 5. Temporal evolutions of the (a) Taylor shape parameter and (b) inclination angle of the initially spherical capsules with SK membrane at $C=100$.

III. RESULTS AND DISCUSSIONS

The transient deformation of spherical and oblate spheroidal capsules in unbounded simple shear flow is studied, under various dimensionless shear rates. The capsules are unstressed at their initial shapes. The internal and external fluids have the same property. Due to the small length scale of the capsule, the initial effect can be neglected. The dimensionless shear rate plays an essential role in determining the capsule deformation. It is defined as $G=\mu ka/E$, where the term μ is the viscosity of the surrounding fluid, k is the shear rate, E is the shear elasticity of the membrane. The term a is the equivalent radius, in the form of $a=(3V/4\pi)^{1/3}$, where the term V is capsule volume.

In the present simulation, the computational domain is a cubic box with side length $10a$. Numerical experiment shows that it is large enough to neglect the boundary effect. The capsule is at the center of the domain, and its membrane is discretized into 8192 flat triangular elements connecting 4098 membrane nodes. The fine mesh block covered from $3a$ to $7a$ in all axes. The other domain was covered with coarse mesh. The grid resolutions in fine and coarse block were $\Delta x_f=\Delta y_f=a/12$ and $\Delta x_c=\Delta y_c=a/6$, respectively. Grid-independent study showed that this mesh density was sufficient.

A. Initially spherical capsules

First studied is the deformation of initially spherical capsules with neo-Hookean membrane. The dimensionless shear rate G ranges from 0.0125 to 0.2. The present results show that after immersed in the flow, a capsule deforms to a steady profile, and then the membrane rotates around the liquid inside (steady tank-treading motion). These are similar to the results reported by Ramanujan and Pozrikidis [11] and Lac *et al.* [31]. For $G=0.05$, the steady deformed capsule and the flow field around the capsule's cross section in the plane of shear are presented in Fig. 3. It is observed that the cross section of the capsule resembles a closed streamline. Recirculating regions are found at two ends of the capsule.

The deformation of the capsule is measured by the Taylor deformation parameter D_{xz}, which is defined as $D_{xz}=(L-B)/(L+B)$, where L and B are the length and width of the capsule in the plane of shear. The temporal evolutions of the capsules' Taylor deformation parameter are presented in Fig. 4(a). It is seen the time taken to achieve steady shape is shorter if the dimensionless shear rate is lower. A lower shear rate means the ratio between elastic and shear forces is larger, thus the capsule only needs to deform a little to generate enough elastic force to balance the viscous shear force. The present results were compared with that of Ramanujan and Pozrikidis [11], in which the same case was studied with the boundary element method. The differences of the results are within 5%. Figure 4(b) presents the temporal evolutions of the capsules' inclination angle (with respect to x axis) in the plane of shear. With the shear rate increasing, the capsules are observed to be more aligned with the flow.

The NH law corresponds to membranes made of polymerized material. The area dilation is unrestricted. For above cases, the maximum membrane area change ranges from 0.4% for $G=0.0125$ to 23.5% for $G=0.2$. The membranes of biological cells are usually incompressible, for example, red blood cells, whose membrane follows SK law. The deformation of initially spherical capsules with SK membrane is studied. The moduli ratio C is chosen to be 100 to take the membrane-area incompressibility into account. For capsules with SK membrane, the steady configuration of the capsule and the time taken to achieve a steady shape depends not only on the dimensionless shear rate, but also on the moduli ratio. A small dimensionless shear rate or a large moduli ratio will restrict the capsule deformation and shorten the time it takes to achieve a steady shape. The temporal evolutions of the capsules' Taylor deformation parameter D_{xz} and the inclination angle are presented in Fig. 5. From the results, it is seen that the overall behavior of the capsules is qualitatively similar to that of capsules with NH membrane. The steady tank-treading mode of the capsule is achieved after an initial transient stage. The membrane area changes for capsules with SK membrane are much smaller than those with NH membrane. At $G=0.3$, the membrane area change is within 1.8%.

B. Initially oblate spheroidal capsules

Perfectly spherical capsules are hardly encountered in practice. In this section, the deformation of oblate spheroidal capsules, with aspect ratios of 10:9, 3:2, and 2:1, is studied under various dimensionless shear rates.

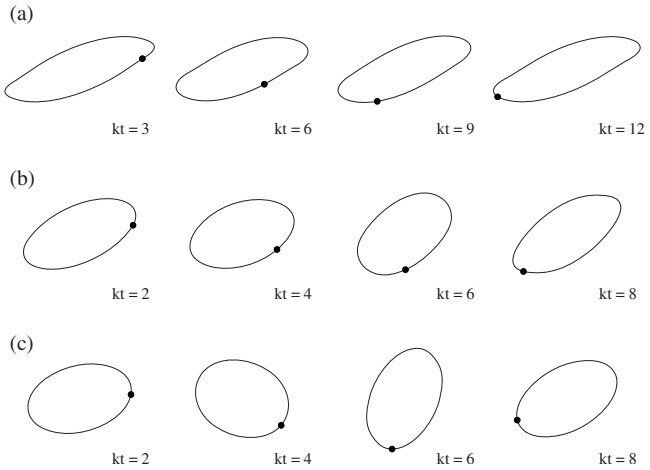

FIG. 6. Membrane profiles in the plane of shear for initially oblate spheroidal capsules with aspect ratio of 3:2. (a) $G=0.2$; (b) $G=0.05$; (c) $G=0.0125$.

First studied is the motion of capsules with NH membrane. From the results, it is observed that at large shear rates, the capsules undergo an unsteady "swinging" motion, in which while the capsules' membranes are rotating around the liquid inside, the capsules undergo periodic shape deformation and inclination oscillation. For a capsule with an aspect ratio of 3:2 at $G=0.2$, its snapshots of the cross section

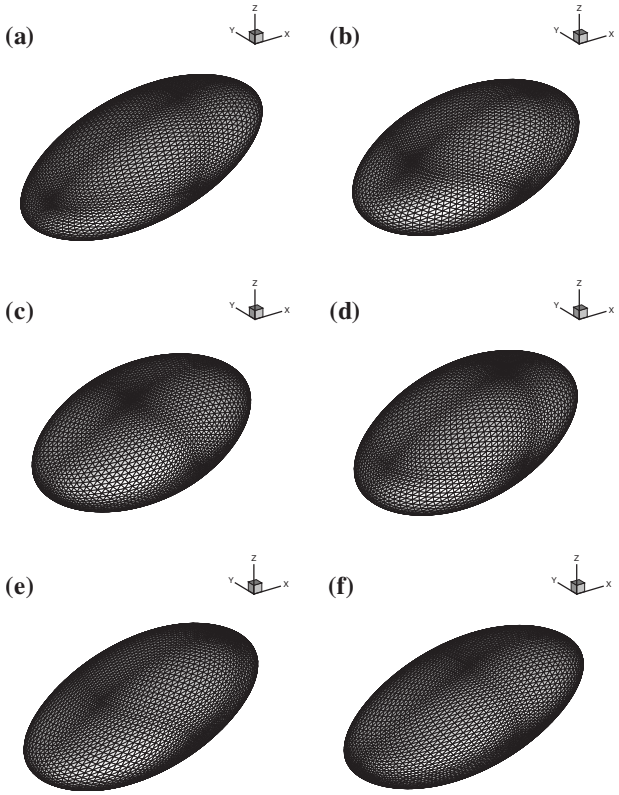

FIG. 7. 3D profiles of the capsule [in Fig. 6(a)] during the swinging motion. The dimensionless time kt=(a) 3, (b) 5, (c) 7, (d) 9, (e) 11, (f) 13.

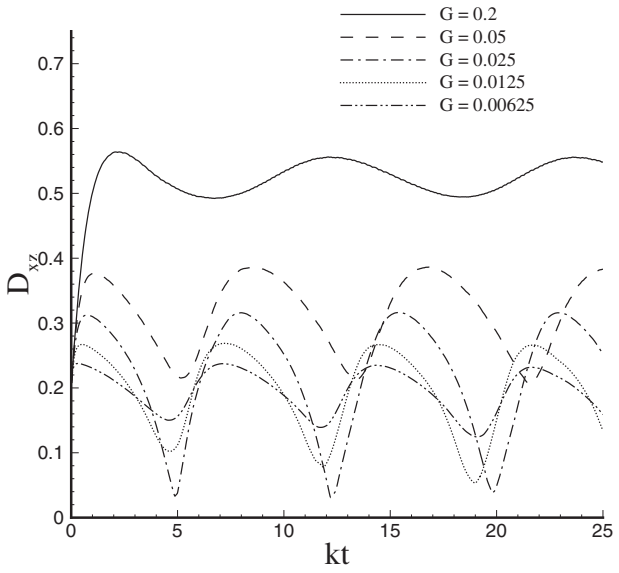

(a)

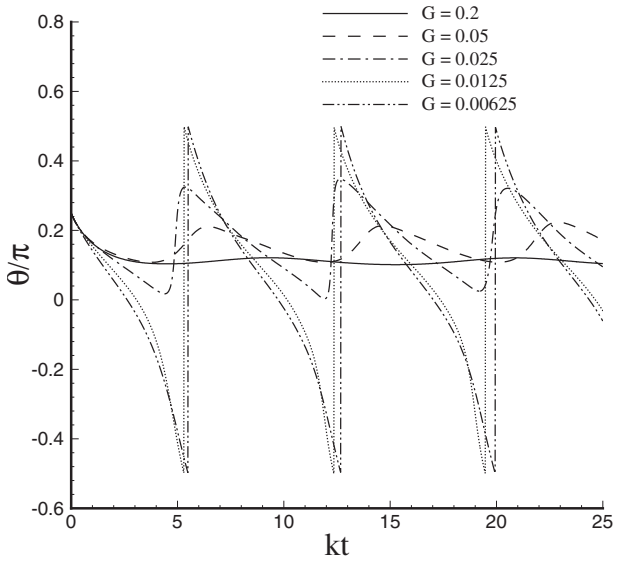

(b)

FIG. 8. Temporal evolutions of the (a) Taylor shape parameter and (b) inclination angle of the initially oblate spheroidal capsules (aspect ratio 3:2) with NH membrane.

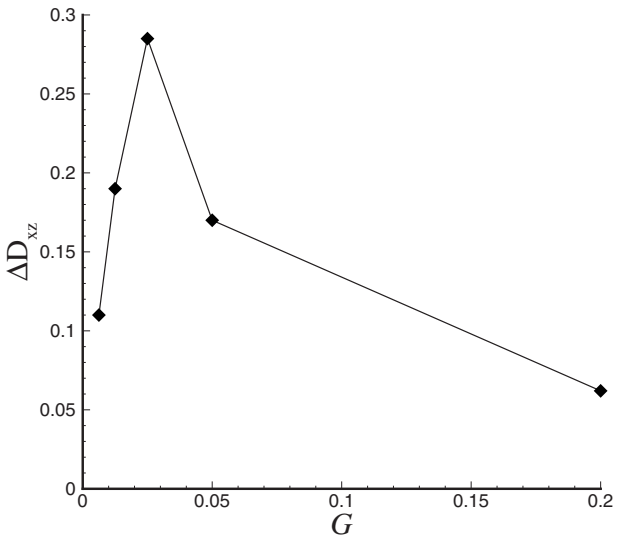

(a)

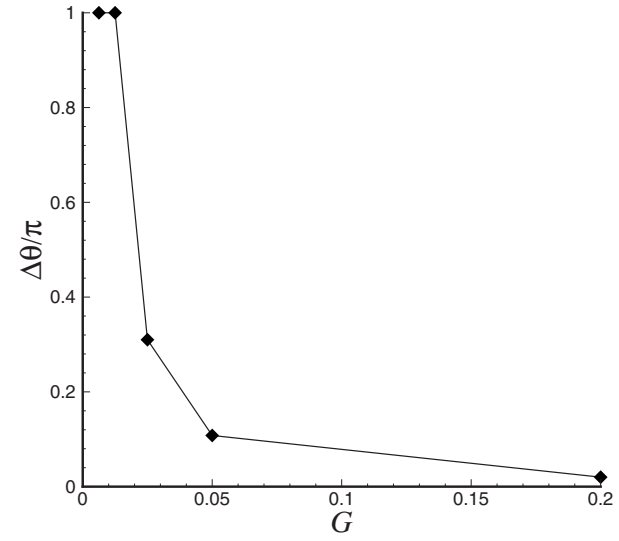

(b)

FIG. 9. Oscillation amplitudes of the (a) Taylor shape parameter and (b) inclination angle of the initially oblate spheroidal capsules (aspect ratio 3:2) with NH membrane.

(in the plane of shear) during the swinging motion are presented in Fig. 6(a). The snapshots of the capsule's 3D profiles are presented in Fig. 7, which gives a clearer illustration of the swinging motion.

The cross sections of the same capsule at $G=0.05$ during the swinging motion are presented in Fig. 6(b). It is seen from the results that the deformation of the capsule is smaller compared with that at $G=0.2$, however, the inclination oscillation amplitude becomes larger. In the experiment of Walter *et al.* [4], the dynamic motion of synthetic microcapsules with polymerized membrane is studied under shear flow conditions. It is found that the capsules undergo a similar swinging motion at large shear rates. It is also observed that as the shear rate decreases, the capsules' inclination oscillation amplitude increases. It is exciting that the present results qualitatively agree with experiment. In the experiment study, the matrix fluid is much more viscous than the liquid inside the capsule. However, the same case cannot be studied by the current method, which can only consider capsules with the internal fluid viscosity similar to that outside.

The shear rate is further decreased: at $G=0.0125$ the snapshots of the same capsule's cross sections are presented in Fig. 6(c). It is quite interesting to find that the capsule's motion has changed from swinging to tumbling.

To give a more quantitative description of the capsules' motion, the temporal evolutions of the capsule's Taylor shape parameter and inclination angle in the plane of shear are presented in Fig. 8. It is seen that the evolution curves un-

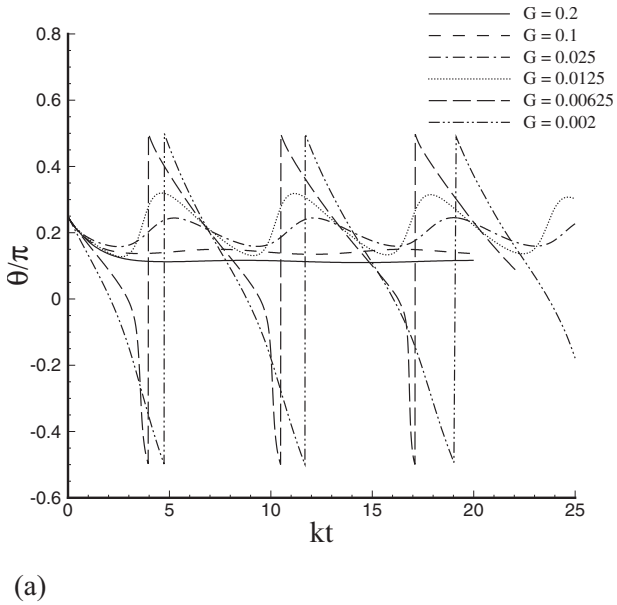

(a)

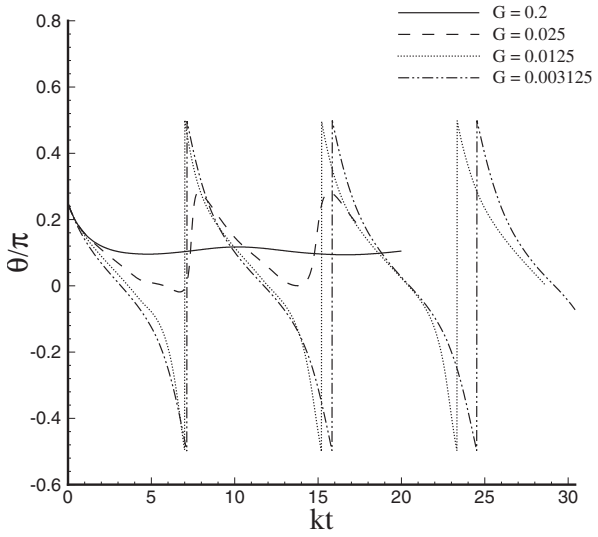

(b)

FIG. 10. Temporal evolutions of the inclination angle of the initially oblate spheroidal capsules with NH membrane, the aspect ratios are (a) 10:9 and (b) 2:1.

dergo oscillations. The oscillation amplitudes of the Taylor shape parameter and inclination angle under different shear rates are presented in Fig. 9. It is found from the results that within the swinging region, the oscillation amplitudes increase with the shear rate decreasing. The mode transition happens between $G=0.025$ and $G=0.0125$, below which the oscillation amplitude the inclination angle equals π, which indicates than the capsule is tumbling.

The dynamic motion of oblate spheroidal capsules, with aspect ratios of 10:9 and 2:1, is also studied under various dimensionless shear rates. The temporal evolutions of the capsules' inclination angle in the plane of shear are presented in Fig. 10. From the results, it is seen that the behavior of the capsules are similar to that of the capsule with aspect ratio of 3:2. With the shear rate decreasing, the capsules' inclination

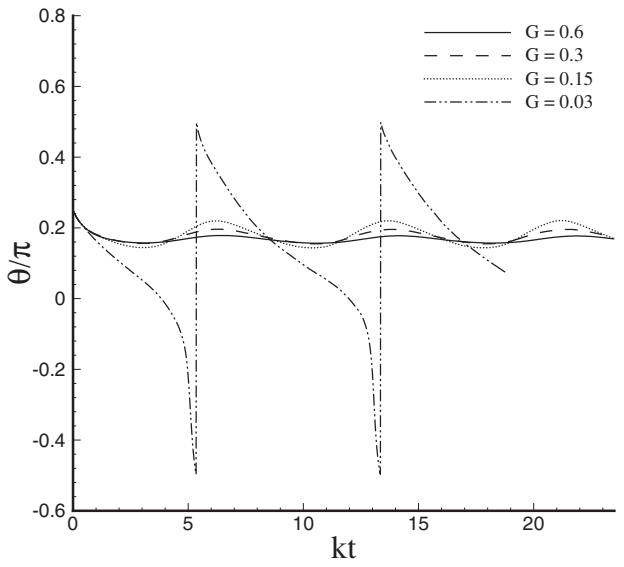

FIG. 11. Temporal evolutions of the inclination angle of the initially oblate spheroidal capsules (aspect ratio 3:2) with SK membrane at $C=100$.

oscillation amplitude increases, and finally triggers the transition from swinging to tumbling.

It must be noted the deformation of oblate spheroidal capsules with NH membrane has been studied by Ramanujan and Pozrikidis [11] with the boundary element method. All shear rates considered in their study falls into the swinging region. Within this region, the present results are comparable to those of Ramanujan and Pozrikidis.

In the recent experiment of Abkarian *et al.* [5] on red blood cells in shear flow, it is observed the cells present an oscillation of their inclination superimposed to the tank-treading motion, and tank-treading-to-tumbling transition can be triggered by decreasing the shear rate. These findings cannot be covered by the well-known theory of Keller and Skalak [8], in which the capsule is assumed to have a fixed ellipsoidal shape with a moving membrane.

It is well known that the membrane of red blood cells is strongly resistant to membrane area dilation. Here, the oblate spheroidal capsules with SK membrane and moduli ratio $C=100$, are employed as a simplified model of the red blood cells. The dynamic motion of capsules with aspect ratios of 10:9, 3:2, and 2:1 is studied. For all cases considered, the shear-rate decreasing induced transition from swinging to tumbling is observed. The temporal evolutions of the inclination angle in the plane of shear are presented in Fig. 11, for the capsule with aspect ratio of 3:2. A similar result is obtained for capsules with aspect ratios of 10:9 and 2:1.

In the theory of Skotheim and Secomb [10], the swinging-to-tumbling transition of an elastic capsule was found to occur via a narrow intermittent regime of successive swinging and tumbling. Abkarian *et al.* also observed this phenomenon in the experiment [5]. In Fig. 12, the temporal evolution of the inclination angle, for a capsule with NH membrane and aspect ratio 3:2, is presented at $G=0.0221$ and 0.0225. It is seen that in the initial stage, the capsule carries out alternate tumbling and swinging motions, which shows some similarities to the intermittent mode of Skotheim and Secomb [10],

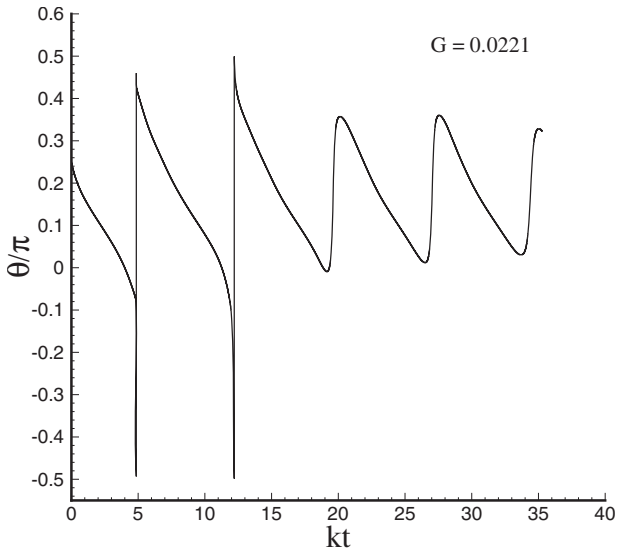

(a)

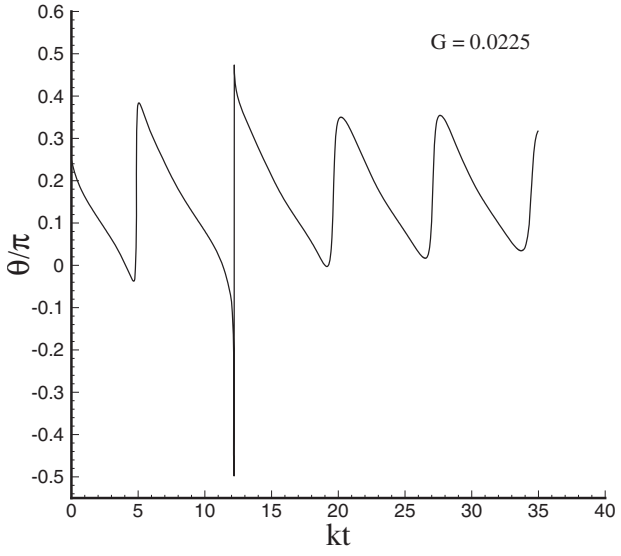

(b)

FIG. 12. Temporal evolutions of the inclination angle of the initially oblate spheroidal capsules (aspect ratio 3:2) with NH membrane at G=(a) 0.0221 and (b) 0.0225.

as well as Abkarian *et al.* [5]. After this initial stage, only swinging motion is observed. Similar behavior has also been observed for elastic capsules with SK membrane and aspect ratios of 10:9 and 2:1. In much longer computation, wrinkles of the membrane due to a lack of bending resistance became severe and the computation results tended to become unreliable. Thus the present simulations may suggest an intermittent motion of the capsules, similar to that of Skotheim and Secomb; however, there is not sufficient evidence in the present study to conclude that the present capsules carried out a steady intermittent motion.

The swinging motion and swinging-to-tumbling transition of capsules, which were observed in recent experiments, could be reproduced by the present numerical model. The present results also show that the theoretical framework of Skotheim and Secomb [10] for a Keller and Skalak type model is applicable to a full 3D simulation.

In the present study, because the immersed boundary method was employed, the simulations were restricted to capsules with the internal fluid viscosity the same as that outside. The undergoing work is to improve the present method by replacing the immersed boundary method with the front-tracking method [32,33], which would relax the constraint that the interior and exterior fluids are of the same viscosity. This would point to a broader application of the numerical studies, for example, to use the observed dynamics to measure capsule properties, or use the simulations to suggest parameter regimes for experiments where the properties can be most sensitively deduced.

IV. CONCLUSION

The dynamic motion of capsules in shear flow is studied by direct numerical simulation. The capsules consist of Newtonian liquid droplets enclosed by elastic membranes with or without considering the membrane-area incompressibility. The dynamic motion of capsules with initially spherical and oblate spheroidal unstressed shapes is studied, under various shear rates. The results show that spherical capsules deform to stationary shapes and achieve steady tank-treading motion. At large shear rates, oblate spheroidal capsules carry out a swinging motion, in which a capsule undergoes periodic shape deformation and inclination oscillation while its membrane is rotating around the liquid inside. With the shear rate decreasing, the capsules' inclination oscillation amplitude increases, and finally triggers the swinging-to-tumbling transition.

ACKNOWLEDGMENT

The authors are grateful to the referees whose comments and suggestions have significantly improved the quality of this paper.

[1] H. L. Goldsmith and J. Marlow, Proc. R. Soc. London, Ser. B **182**, 351 (1972).
[2] T. M. Fischer, M. Stöhr-Liesen, and H. Schmid-Schönbein, Science **202**, 894 (1978).
[3] S. Chien, Annu. Rev. Physiol. **49**, 177 (1987).
[4] A. Walter, H. Rehage, and H. Leonhard, Colloids Surf., A **183-185**, 123 (2001).
[5] M. Abkarian, M. Faivre, and A. Viallat, Phys. Rev. Lett. **98**, 188302 (2007).
[6] D. Barthès-Biesel, J. Fluid Mech. **100**, 831 (1980).

[7] D. Barthès-Biesel and J. M. Rallison, J. Fluid Mech. **113**, 251 (1981).
[8] S. R. Keller and R. Skalak, J. Fluid Mech. **120**, 27 (1982).
[9] C. Misbah, Phys. Rev. Lett. **96**, 028104 (2006).
[10] J. M. Skotheim and T. W. Secomb, Phys. Rev. Lett. **98**, 078301 (2007).
[11] S. Ramanujan and C. Pozrikidis, J. Fluid Mech. **361**, 117 (1998).
[12] C. D. Eggleton and A. S. Popel, Phys. Fluids **10**, 1834 (1998).
[13] J. Beaucourt, F. Rioual, T. Séon, T. Biben, and C. Misbah, Phys. Rev. E **69**, 011906 (2004).
[14] H. Noguchi and G. Gompper, Phys. Rev. Lett. **93**, 258102 (2004).
[15] H. Noguchi and G. Gompper, Phys. Rev. E **72**, 011901 (2005).
[16] H. Noguchi and G. Gompper, Phys. Rev. Lett. **98**, 128103 (2007).
[17] Y. Sui, Y. T. Chew, P. Roy, X. B. Chen, and H. T. Low, Phys. Rev. E **75**, 066301 (2007).
[18] R. Skalak, A. Tozeren, R. P. Zarda, and S. Chien, Biophys. J. **13**, 245 (1973).
[19] Y. Peng, C. Shu, Y. T. Chew, X. D. Niu, and X. Y. Lu, J. Comput. Phys. **218**, 460 (2006).
[20] Y. Sui, Y. T. Chew, P. Roy, and H. T. Low, Int. J. Numer. Methods Fluids **53**, 1727 (2007).
[21] C. S. Peskin, J. Comput. Phys. **25**, 220 (1977).
[22] C. S. Peskin, Acta Numerica **11**, 479 (2002).
[23] S. Chen and G. D. Doolen, Annu. Rev. Fluid Mech. **30**, 329 (1998).
[24] D. Yu, R. Mei, L. Luo, and W. Shyy, Prog. Aerosp. Sci. **39**, 329 (2003).
[25] A. J. C. Ladd, J. Fluid Mech. **271**, 285 (1994).
[26] A. J. C. Ladd, J. Fluid Mech. **271**, 311 (1994).
[27] D. Yu and S. S. Girimaji, Physica A **362**, 118 (2006).
[28] J. M. Charrier, S. Shrivastava, and R. Wu, J. Strain Anal. Eng. Des. **24**, 55 (1989).
[29] S. Shrivastava and J. Tang, J. Strain Anal. Eng. Des. **28**, 31 (1993).
[30] Z. L. Guo, C. G. Zheng, and B. C. Shi, Phys. Rev. E **65**, 046308 (2002).
[31] E. Lac, D. Barthes-Biesel, N. A. Pelekasis, and J. Tsamopoulos, J. Fluid Mech. **516**, 303 (2004).
[32] S. O. Unverdi and G. Tryggvason, J. Comput. Phys. **100**, 25 (1992).
[33] P. Lallemand, L. Luo, and Y. Peng, J. Comput. Phys. **226**, 1367 (2007).